Boundary-Layer Meteorol (2016) 158:473–488
DOI 10.1007/s10546-015-0096-7

NOTES & COMMENTS

Estimation from Soil Temperature of Soil Thermal Diffusivity and Heat Flux in Sub-surface Layers

Kedong An[1] · Wenke Wang[1] · Yaqian Zhao[2] · Wenfeng Huang[1] · Li Chen[1] · Zaiyong Zhang[1] · Qiangmin Wang[1] · Wanxin Li[1]

Received: 16 February 2015 / Accepted: 22 September 2015 / Published online: 15 October 2015

Abstract Soil thermal parameters are important for calculating the surface energy balance and mass transfer. Previous studies have proposed methods to estimate thermal parameters using field data; however, the application of these methods lacks validation and comprehensive evaluation under different climatic conditions. Here, we evaluate four methods (amplitude, phase shift, conduction–convection and harmonic) to estimate thermal diffusivity (k) under different climatic conditions. Heat flux was simulated and compared with data from heat-flux plates to validate the application of the four methods. The results indicated that, under clear-sky conditions, the harmonic method had the greatest accuracy in estimating k, though it generated large errors on rainy days or under overcast conditions. The conduction–convection method (CCM) provided a reliable estimate of k on rainy days, or under overcast skies, coinciding with increased water movement in the soil profile. The amplitude method, although a simple calculation, had poor accuracy for rainy and overcast conditions. Finally, the phase shift method was shown to be a suitable alternative for CCM to estimate k under overcast conditions, though only when soil moisture content was high.

Keywords Conduction–convection method · Harmonic method · Heat flux · Soil Temperature · Soil thermal diffusivity

1 Introduction

Information on soil thermal properties (thermal conductivity λ, thermal diffusivity k and volumetric heat capacity c_v) is required to accurately predict soil temperatures, and to evaluate its influence on the surface energy balance (Heusinkveld et al. 2004; Alkhaier et al. 2012),

✉ Wenke Wang
wenkew@gmail.com

1 Key Laboratory of Subsurface Hydrology and Ecological Effects in Arid Region, Chang'an University, Ministry of Education, Xi'an, People's Republic of China

2 UCD Dooge Centre for Water Resources Research, School of Civil, Structural, and Environmental Engineering, University College Dublin, Newstead, Belfield, Dublin 4, Ireland

unsaturated hydraulic conductivity (Hopmans and Dane 1986; Andry et al. 2009), and soil water vapour flow in the coupling of water and heat transfer (Saito et al. 2006; Bittelli et al. 2008; Wang et al. 2011a, b, 2012a, b; Zhang et al. 2015).

Generally, λ and k are related as $\lambda = kc_v$, which can easily be deduced from soil components, therefore only λ or k needs to be determined (Van Wijk 1963; Verhoef et al. 1996). Thermal parameters of a soil depend on several factors, such as soil texture, mineralogical composition, the presence of salt, soil moisture content (Kunii and Smith 1960; Riha et al. 1980; Campbell 1985; Noborio and McInnes 1993; Wang et al. 2005; Liu et al. 2008), therefore making estimations of thermal parameters difficult. Many researchers have attempted to parametrize λ or k for certain soils by using soil moisture content, density and shape factors under laboratory conditions (De Vries 1956; Abu-Hamdeh and Reeder 2000; Zhao et al. 2009). However, due to scale effects (Barrios and Francés 2012) and the complex effects of soil shape, particle size and packing (Evett et al. 2012), errors are often generated when the laboratory results are extrapolated to field experiments.

In order to avoid these errors, methods have been developed to estimate k using field data on soil temperature (Horton and Wierenga 1983; Verhoef et al. 1996; Heusinkveld et al. 2004). If the soil is homogeneous, the analytical solutions of a one-dimensional soil conductive equation can be used to estimate k using the amplitude method, phase shift method, arctangent, logarithmic and harmonic methods. The amplitude and the phase methods use a single sinusoidal temperature wave (Sellers 1965) while the arctangent and the logarithmic methods use two harmonics (Nerpin et al. 1972). Horton and Wierenga (1983) proposed the harmonic method to estimate k with a series of harmonics accurately describing the surface temperature. All of these methods are based on the assumption of a conductive heat equation with a constant k during a single day. However, heat transfer in the soil contains not only heat conduction but also heat convection (de Silans et al. 1996; Gao et al. 2003), both of which contribute to soil temperature changes in the soil. Based on this theory, Gao et al. (2003) proposed a new method to estimate k by deducing the analytical solution to the equation for one-dimensional thermal conduction and convection using the harmonic method and the Laplace transform method (Gao 2005). Wang et al. (2012a, b) improved the solution of the conduction and convection equation with a boundary soil temperature being described as a Fourier series instead of a single sine wave. The Fourier series model yields a better estimation of soil temperature than does the single sine wave model.

So far, many researchers have attempted to estimate k via the above models and approaches using field data despite quite different weather conditions. Dai et al. (2009) used the conduction–convection method (CCM) and harmonic method to estimate k using soil temperature data, although only seven days of data under clear skies were used. Wang et al. (2010) compared six methods to determine k in the Loess Plateau of China under a single weather condition. Otunla and Oladiran (2013) assessed the performances of six methods to estimate k in both dry and wet seasons in West Africa, but this investigation used similar weather conditions. The accuracy of these investigations was assessed by evaluating the error between observed and simulated temperatures by the estimated k, these being deduced from soil temperature profiles in the same period. Miao et al. (2012) tried to use the heat flux to assess the amplitude, the phase shift, the conduction–convection, and the harmonic methods to estimate k, but only 5 days of data collected under clear-sky conditions. Overall, the application of these methods to estimating k lacks comprehensive and systematic validation by long-term field data under different weather conditions.

The aim of this paper is to identify the best method for estimating k in a semi-arid area under different weather conditions. In order to accurately parametrize k, measurements of soil temperature, moisture content and heat flux are used. Four common methods (ampli-

tude, phase shift, conduction–convection and harmonic) were used to estimate k and their application validated by comparing the estimated heat flux with observations from heat-flux plates under different weather conditions.

2 Theory

The soil heat flux at depth z is given by the Fourier law of heat conduction (Carslaw and Jaeger 1959),

$$G = \lambda \frac{\partial T}{\partial z}, \tag{1}$$

where G (W m^{-2}) is the soil heat flux, λ (W m^{-1} K^{-1}) is the thermal conductivity, T (K) is the soil temperature and z (m) is the depth from the soil surface. The vertical one-dimensional heat conduction equation in an isotropic medium is (Horton and Wierenga 1983),

$$\frac{\partial T}{\partial t} = \frac{1}{c_v} \frac{\partial}{\partial z} \left(\lambda \frac{\partial T}{\partial z} \right), \tag{2}$$

where t (s) is time and c_v (J m^{-3} K^{-1}) is the volumetric heat capacity.

Assuming that both c_v and λ are independent of depth, then the soil thermal diffusivity $k = \lambda / c_v$ (m^{2}s^{-1}) is a constant, so Eq. 2 becomes,

$$\frac{\partial T}{\partial t} = k \frac{\partial^2 T}{\partial z^2}. \tag{3}$$

2.1 Amplitude Method and Phase Shift Method

Soil temperature measured at any depth can be described by a sine wave (Verhoef et al. 1996), so the temperature at z_1 and z_2 can be expressed as,

$$T(z_1, t) = \overline{T}(z_1) + A_1 \sin(\omega t + \varphi_1), \tag{4}$$

$$T(z_2, t) = \overline{T}(z_2) + A_2 \sin(\omega t + \varphi_2), \tag{5}$$

where $\overline{T}(z_1)$ and $\overline{T}(z_2)$ are the average soil temperatures at depths z_1 and z_2, respectively, A_1, A_2, φ_1 and φ_2 are the temperature amplitudes and phase shifts at depths z_1 and z_2, respectively. These six parameters can be calibrated from the temperature observations using the least-squares method. Additionally, ω (rad s^{-1}) is the rotational angular velocity of the earth: $\omega = \frac{2\pi}{p}$ with p (24 h) denoting the period of the fundamental cycle.

Soil thermal diffusivity can therefore be deduced using the amplitude and the phase shift methods, viz.

$$k_A = \frac{\omega (z_1 - z_2)^2}{2[\ln(A_1/A_2)]^2}, \tag{6}$$

$$k_P = \frac{\omega (z_1 - z_2)^2}{2(\varphi_1 - \varphi_2)^2}. \tag{7}$$

Using Eq. 4 as the upper boundary, the solution of Eq. 3 can be deduced as (Carslaw and Jaeger 1959),

$$T(z, t) = \overline{T}(z) + A_1 \exp[-B(z - z_1)] \sin[\omega t + \varphi_1 - B(z - z_1)], \tag{8}$$

where $\overline{T}(z)$ is the average soil temperature at depth z and $B = \sqrt{\omega/2k}$ corresponds to the depth to which the signal propagates during a period of $p = 24$ h (Van Wijk 1963). Combining Eqs. 1 and 8, the heat flux at depth z can be calculated as,

$$G_s(z,t) = kc_v \frac{\Delta T}{\Delta z} + kc_v \sum_{i=1}^{n} \sqrt{2} A_1 B \exp\left[-B(z-z_1)\right] \sin\left[\omega t + \varphi_1 + \frac{\pi}{4} - B(z-z_1)\right], \tag{9}$$

where $\Delta T/\Delta z$ is the gradient of the averaged soil temperature.

2.2 Harmonic Method

Assuming that soil temperatures measured at the upper boundary can be described by a Fourier series (Verhoef et al. 1996), then,

$$T(0,t) = \overline{T}(0) + \sum_{i=1}^{n} A_i \sin(i\omega t + \varphi_i), \tag{10}$$

where $\overline{T}(0)$ is the mean temperature at the soil surface, and A_i and φ_i are the amplitude and phase shift of harmonic i, respectively.

Provided φ_i is constant, the analytical solution of Eq. 3 for a semi-infinite soil profile is (Carslaw and Jaeger 1959),

$$T(z,t) = \overline{T}(z) + \sum_{i=1}^{n} A_i \exp(-B_i z) \sin(i\omega t + \varphi_i - B_i z), \tag{11}$$

where $B_i = \sqrt{i\omega/2k}$, which corresponds to the depth to which the signal propagates during a period of p/i (Van Wijk 1963).

Using Eq. 10, the soil thermal diffusivity k can be estimated by a least-squares best fit of the calculated temperature to the observed temperature at depth z. Combining Eqs. 1 and 11, soil heat flux can therefore be calculated as,

$$G_s(z,t) = kc_v \frac{\Delta T}{\Delta z} + kc_v \sum_{i=1}^{n} A_i \sqrt{2} B_i \exp\left[-B_i(z-z_1)\right] \sin\left[i\omega t + \varphi_i + \frac{\pi}{4} - B_i(z-z_1)\right]. \tag{12}$$

2.3 Conduction–Convection Method (CCM)

The general heat transfer equation assumes that soil thermal conductivity and diffusivity are independent of depth. In fact, as highlighted by de Silans et al. (1996), the soil moisture content that affects soil thermal parameters varies depending on time and depth. Therefore, Gao et al. (2003) and Gao (2005) incorporated thermal conduction and convection equations considering the influence of soil moisture content as, viz.

$$\frac{\partial T}{\partial t} = k \frac{\partial^2 T}{\partial z^2} + W \frac{\partial T}{\partial z}, \tag{13}$$

where W is equal to the sum of the vertical gradient of soil diffusivity and the liquid water flux density. The analytical solution of Eq. 13 with the boundary conditions given by Eq. 4 with a sine wave is (Gao et al. 2003),

$$T(z,t) = T_0 + A\exp\left[\left(-\frac{W}{2k} - \frac{\sqrt{2}}{4k}\sqrt{W^2+\sqrt{W^4+16k^2\omega^2}}\right)z\right] \times \sin\left[\omega t - z\frac{\sqrt{2}\omega}{\sqrt{W^2+\sqrt{W^4+16k^2\omega^2}}}\right]. \quad (14)$$

The soil thermal diffusivity deduced using CCM, therefore, is

$$k = -\frac{\omega(z_1-z_2)^2\ln(A_1/A_2)}{(\varphi_1-\varphi_2)\left[(\varphi_1-\varphi_2)^2+\ln^2(A_1/A_2)\right]}. \quad (15)$$

Combining Eqs. 1 and 14, the heat flux can therefore be calculated using the observed temperature,

$$G_s(z,t) = kc_v\frac{\Delta T}{\Delta z} + kc_v MA_1\exp\left[-M(z-z_1)\right]\times\sin\left[\omega t+\varphi_1-N(z-z_1)\right] - NA_1\exp\left[-M(z-z_1)\right]\times\cos\left[\omega t+\varphi_1-N(z-z_1)\right], \quad (16)$$

where $M = \frac{W}{2k} + \frac{\sqrt{2}}{4k}\sqrt{W^2+\sqrt{W^4+16k^2\omega^2}}$ and $N = \frac{\sqrt{2}\omega}{\sqrt{W^2+\sqrt{W^4+16k^2\omega^2}}}$.

2.4 Heat Flux Estimated by the Gradient Method

Apart from the methods mentioned above, the one-dimensional soil heat flux for a homogeneous medium is described by the gradient method (Horton and Wierenga 1983; Evett et al. 2012),

$$G_i^* = kc_v\left(\frac{T_{i,j}-T_{i,j-1}}{z_{i,j}-z_{i,j-1}}\right), \quad (17)$$

where i is the time index and j is the depth index.

3 Field Experiments

The field experiment was conducted at the semi-arid Groundwater and Environment site located at Chang'an University, Xi'an, China (34.28′N, 108.93′E). There were 12 observation wells arranged in two rows, where one row was bare soil and the other was planted with salix (Fig. 1). All of the wells had the same diameter (1 m) and the same height from the ground. The water table depths were approximately 0.5, 1, 2, 3, 4 and 5 m, respectively. The soil was homogeneous silty sand, with moderately large heat and water capacities (0.06–0.34 $m^3\ m^{-3}$) obtained from the Maowusu Dessert in the north-west of China.

The soil temperature was measured at depths of zero, 0.05, 0.1, 0.2, 0.3 and 0.6 m with thermocouple probes (Campbell Scientific Inc., $\pm 3 \sim 5$ %), while soil moisture content was measured at a depth of 30 mm with $ECH_2O - 5TM$ (Decagon Inc., $\pm 1 \sim 2$ %), and heat flux was measured with heat-flux plates (Hukeflux Inc., $\pm 5 \sim 10$ %) at depths of 0.03 m and 0.075 m. Groundwater table was monitored with DI501 (Diver Inc., ± 0.05 %). All data were automatically recorded every 10 min via a data logger (CR-3000, Campbell).

A standard meteorological station, situated 1 m from the trial plot recorded every 10 min the net radiation, air temperature, pressure, precipitation, evaporation, relative humidity, wind speed and wind direction at a height of 1.5 m and CO_2 concentrations at a height of 2 m.

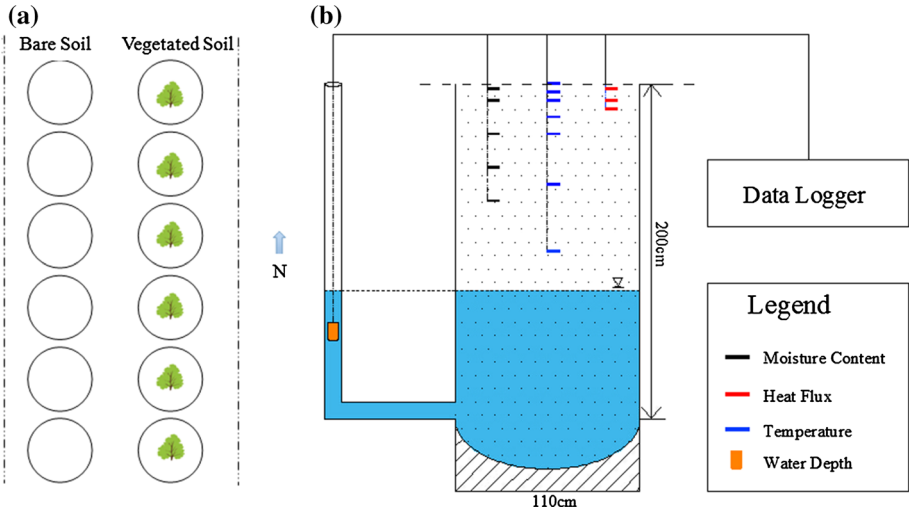

Fig. 1 **a** Plan of observation wells with different water-table depth of 0.5, 1, 2, 3, 4 and 5 m (from north to south) in the trial plot; and **b** side elevation of sensor locations in the observation well with a water table of 2 m

4 Results and Discussion

In this experiment, data from a well with the water depth of 2 m during the 2014 summer season, from August 21 to October 22, were collected to assess the application of the four methods to estimate the thermal diffusivity over bare soil. Due to instrument malfunctions and emergency shutdowns, soil temperatures were not available from August 28 to August 30, from September 9 to September 22, and from October 10 to October 15.

Figure 2 shows the temporal variations of precipitation, air temperature, soil moisture content at 0.03 m, and soil heat flux at 0.03 m and 0.075 m, while Fig. 3 shows the soil profile temperature in the observation well. The soil temperature at different depths showed a typical and steady sine behaviour with the amplitude decreasing and the phase shift being in hysteresis as the depth increased. Although the decreasing amplitude in the soil profile is intriguing, this is not discussed further.

On a rainy day or on a day with severe convective weather, the sub-surface soil temperature frequently showed an unsteady sine-like behaviour. For example, on September 23, the soil temperature at zero and 0.05 m depths recorded two peaks. At the same time, the amplitude of heat flux at 0.03 m was also much smaller than that at 0.075 m, this being similar to the soil temperature profile. More specifically, the distribution of heat flux at 0.03 m was scattered. One possible reason for this relates to the sub-surface heat flux depending not only on soil moisture content, but also on meteorological factors, such as wind speed (Miao et al. 2012). It is worth noting that the soil moisture content at 0.03 m responds rapidly to precipitation.

In order to assess the four methods to estimate k, and to investigate their application, observations were classified by: clear sky, rainy, and overcast according to precipitation and cloud cover provided locally. Depending on the degree of soil wetness, overcast conditions were classified by two factors: high soil moisture content with low water movement in the soil profile (overcast 1), and low soil moisture content with high water movement in the soil profile (overcast 2). Therefore, four kinds of weather conditions were classed in our investigation.

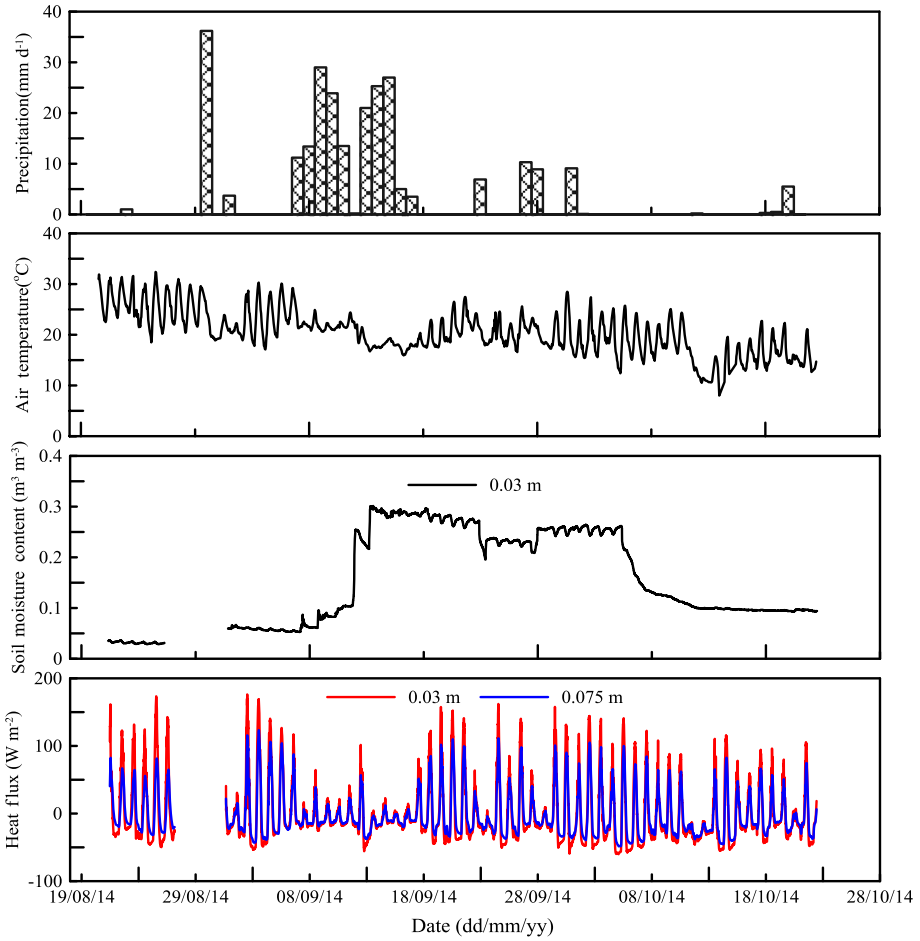

Fig. 2 Diurnal variation of precipitation, air temperature, soil moisture content at 0.03 m, and heat flux at 0.03 and 0.075 m in the observation well

4.1 Soil Thermal Diffusivity Calculations

In order to estimate thermal diffusivity, the observed soil temperatures were fitted to the form of Eqs. 4 and 10, respectively, using a least-squares method based on a MATLAB program. Table 1 presents the coefficient of determination (R^2) under four climatic conditions, with large value of R^2 indicating a good fit.

During the fitting process, only one sine wave (Eq. 4) was used in the amplitude/phase shift/conduction–convection methods while a Fourier series (Eq. 10) was used in the harmonic method to balance the accuracy demands and the calculation simplicity (Miao et al. 2012). Compared with a sine wave, a Fourier series produced higher R^2 regardless of the weather conditions. In the calculation, accordingly, we are more likely to obtain a better fitting curve with a Fourier series due to increased data, as highlighted by Horton and Wierenga (1983). In addition, R^2 for clear-sky conditions is higher than that for rainy or overcast conditions.

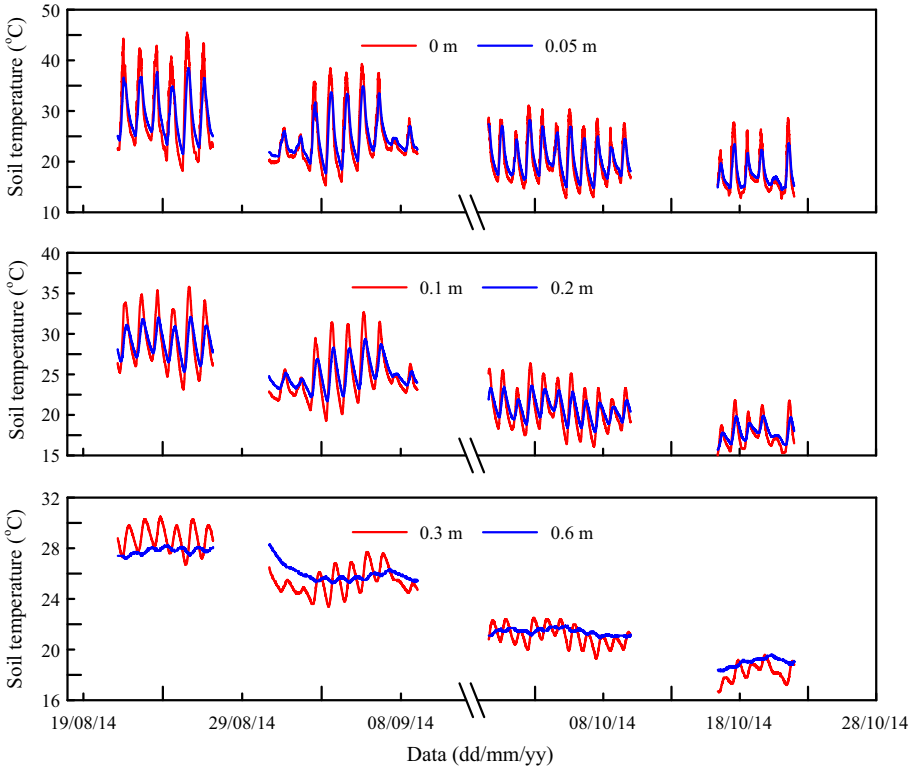

Fig. 3 Diurnal variation of soil temperature at six different depths in the observation well

Table 1 Coefficient determination (R^2) of the measured temperature in the fitting process using a least-squares method

Depth (mm)	Amplitude/phase shift/CCM				Harmonic			
	Clear sky	Rainy	Overcast 1	Overcast 2	Clear sky	Rainy	Overcast 1	Overcast 2
0	0.88	0.70	0.79	0.85	0.97	0.89	0.96	1.0
50	0.92	0.87	0.83	0.87	0.99	0.99	0.99	0.99
100	0.94	0.90	0.86	0.89	0.99	0.99	0.99	1.0

Overcast 1: overcast conditions with high soil moisture content and low water movement in the soil profile; Overcast 2: overcast conditions with low soil moisture content and high water movement in the soil profile

As shown in Table 2, the mean k in the soil profile was calculated using four methods (amplitude, phase shift, conduction–convection and harmonic) under four weather conditions. Generally, k for the silty sand differed at different depths and under different weather conditions with a range of $10^{-5} \sim 10^{-7}$ m^2 s^{-1}. Wang et al. (2010) estimated k of a medium loam to be about 10^{-7} m^2 s^{-1} under clear skies and Otunla and Oladiran (2013) calculated k of a loamy sand to be about $2.5 \sim 8.4 \times 10^{-7}$ m^2 s^{-1}. Liu et al. (2008), using heat-flux data in the field for a long time period, stated that k of a sandy soil with a slight chernozem was $1.4\ (\pm 0.5) \times 10^{-7}$ m^2 s^{-1}.

Table 2 k ($m^2\ s^{-1}$) at different depths by four methods under four typical weather conditions

Weather condition/depth (m)	Amplitude	Phase shift	CCM	Harmonic
Clear sky				
0–0.05	6.5×10^{-7}	6.0×10^{-7}	6.0×10^{-7}	6.0×10^{-7}
0.05–0.1	1.2×10^{-6}	1.0×10^{-6}	1.0×10^{-6}	9.5×10^{-7}
0.1–0.2	1.0×10^{-6}	9.7×10^{-7}	9.7×10^{-7}	9.9×10^{-7}
0.2–0.3	9.3×10^{-7}	9.8×10^{-7}	9.6×10^{-7}	9.3×10^{-7}
0.3–0.6	8.0×10^{-7}	2.1×10^{-6}	1.7×10^{-6}	7.3×10^{-7}
Rainy				
0–0.05	6.8×10^{-7}	1.5×10^{-6}	9.8×10^{-7}	1.0×10^{-6}
0.05–0.1	8.0×10^{-7}	7.8×10^{-7}	7.4×10^{-7}	1.4×10^{-6}
0.1–0.2	4.6×10^{-6}	8.0×10^{-7}	7.3×10^{-7}	6.6×10^{-6}
0.2–0.3	8.8×10^{-5}	3.3×10^{-6}	1.7×10^{-6}	1.7×10^{-5}
0.3–0.6	1.2×10^{-5}	1.5×10^{-6}	1.3×10^{-6}	1.4×10^{-6}
Overcast 1				
0–0.05	6.6×10^{-7}	6.8×10^{-7}	6.6×10^{-7}	8.9×10^{-7}
0.05–0.1	7.5×10^{-7}	7.5×10^{-7}	7.5×10^{-7}	8.8×10^{-7}
0.1–0.2	7.2×10^{-7}	7.2×10^{-7}	7.2×10^{-7}	8.0×10^{-7}
0.2–0.3	6.4×10^{-7}	6.5×10^{-7}	6.4×10^{-7}	7.2×10^{-7}
0.3–0.6	5.2×10^{-7}	5.2×10^{-7}	5.2×10^{-7}	5.3×10^{-7}
Overcast 2				
0–0.05	5.8×10^{-7}	5.9×10^{-7}	5.8×10^{-7}	6.4×10^{-7}
0.05–0.1	7.6×10^{-7}	7.6×10^{-7}	7.6×10^{-7}	8.5×10^{-7}
0.1–0.2	6.6×10^{-7}	6.6×10^{-7}	6.6×10^{-7}	7.6×10^{-7}
0.2–0.3	5.3×10^{-7}	5.5×10^{-7}	5.3×10^{-7}	7.0×10^{-7}
0.3–0.6	8.8×10^{-7}	9.0×10^{-7}	8.8×10^{-7}	1.1×10^{-6}

4.2 Heat Flux

In order to assess the accuracy of k estimated from the amplitude, phase shift, conduction–convection and harmonic methods, the heat flux was introduced herein to be the evaluation standard. If the organic content in the soil is low enough to be ignored, the volumetric heat capacity c_v is a single-valued function of soil moisture content θ ($m^3\ m^{-3}$) at a certain soil bulk density ρ_b (mg m^{-3}) (De Vries 1956; Abu-Hamdeh and Reeder 2000). In this investigation, c_v for the silty sand with particle density of 1.55 mg m^{-3} can be calculated using

$$c_v = 4.18\theta + 0.85\rho_b. \tag{18}$$

Figure 4 shows the observed heat flux (G_m) and simulated heat flux (G_s) at 0.03-m depths using amplitude, phase shift, conduction–convection and harmonic methods. It can be seen that the simulated results are generally representative of the observed heat flux although G_s has a slight deviation from G_m during nighttime. However, G_s estimated by the amplitude and the phase shift methods, has a poor agreement with G_m from September 23 to October 6,

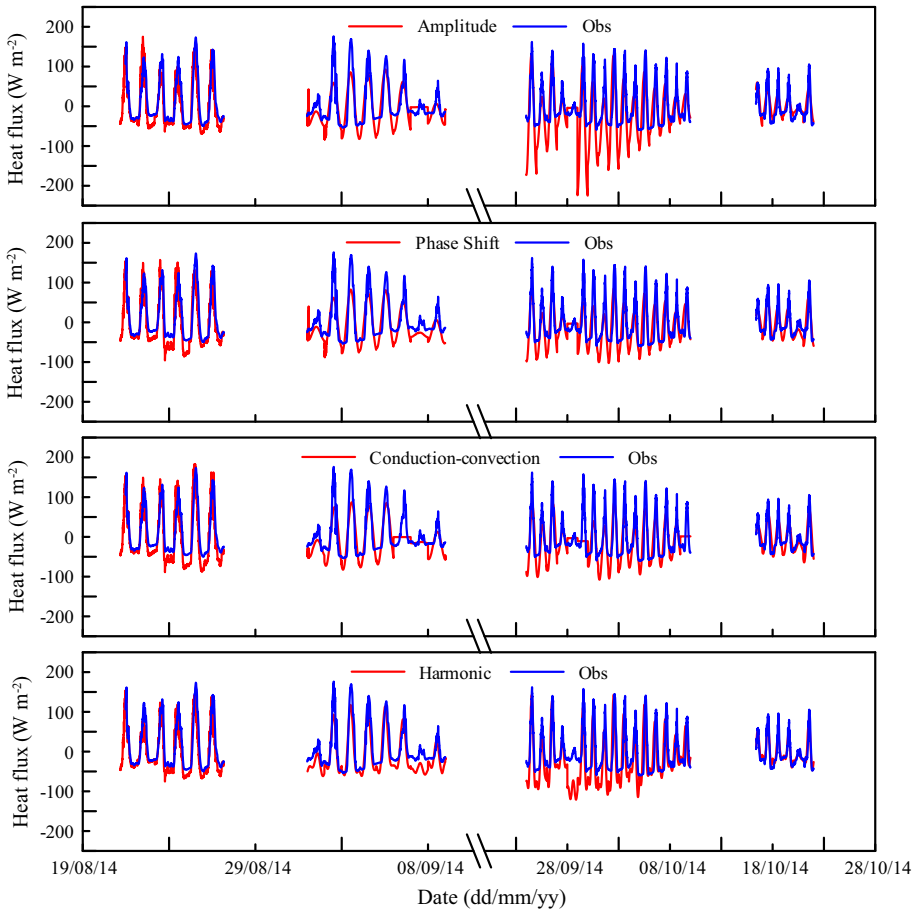

Fig. 4 Temporal variation of soil heat flux estimated by the four methods (amplitude, phase shift, conduction–convection and harmonic) and observed by the heat-flux plates at 0.03 m depth

when soil moisture content was high after a long period of precipitation (Fig. 2). Therefore, the amplitude and the phase shift methods should not be used to estimate k in rainy or overcast conditions with high soil moisture content.

In order to investigate the influence of weather conditions and soil moisture content on the accuracy of the estimated k, the measured and simulated heat fluxes using amplitude, phase shift, conduction–convection and harmonic methods under typical weather conditions were chosen and are presented in Fig. 5.

The relative root-mean-square error *(rRMSE)* of the heat flux was calculated with the four methods, and shown in Table 3. The *rRMSE* is defined as (Lin and Chen 2004),

$$rRMSE = \sqrt{\frac{1}{n}\sum_{i=1}^{n}\left(\frac{G_s - G_m}{G_m}\right)^2}, \tag{19}$$

where i is the dummy variable and n is the number of data elements in the period.

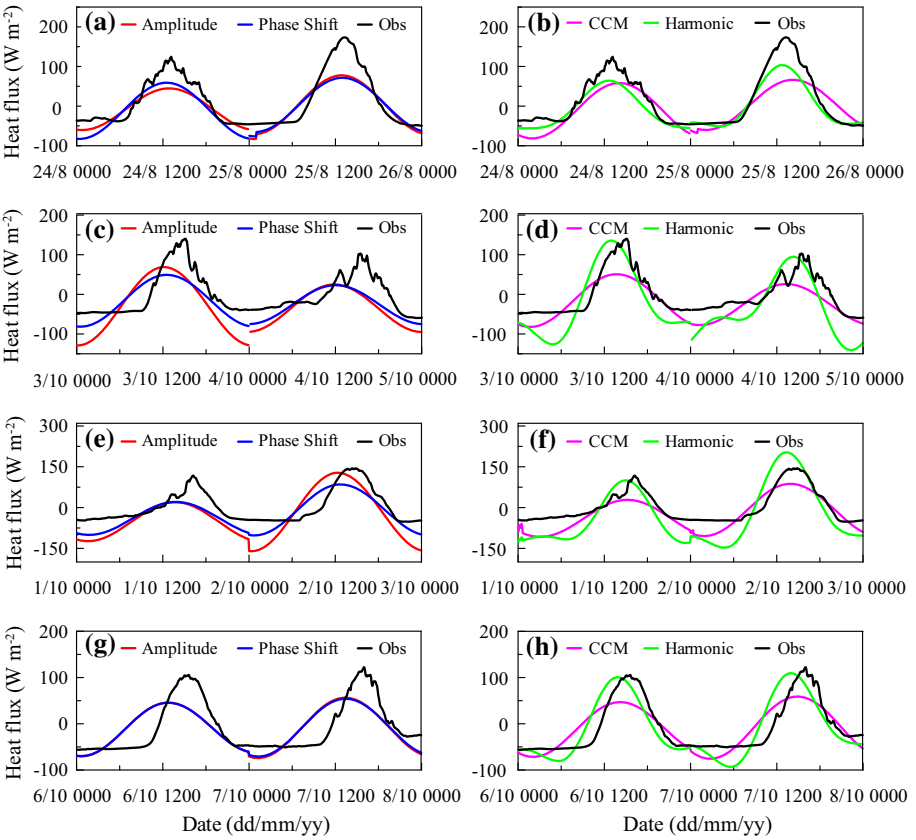

Fig. 5 Soil heat flux estimated by the four methods and observed by heat-flux plates at 0.03 m: **a**, **b** under clear conditions; **c**, **d** on rainy days; **e**, **f** under overcast conditions with high soil moisture content and low water movement in the soil profile; and **g**, **h** under overcast conditions with low soil moisture content and high water movement in the soil profile

Table 3 *rRMSE* of the heat flux G_s estimated by amplitude, phase shift, conduction–convection and harmonic methods against the observation at 30 mm depth

Weather/method	Amplitude	Phase shift	CCM	Harmonic
Clear sky	1.05	1.17	2.22	1.03
Rainy	4.64	3.44	1.31	3.99
Overcast 1	2.09	1.72	1.00	2.38
Overcast 2	2.13	2.04	1.60	2.70

Although some underestimation of heat flux occurred, simulations using the four methods were generally good for clear-sky conditions. More specifically, the harmonic method was visually closest to the measurements in Fig. 5, and also had the lowest *rRMSE* (Table 3). A more accurate k is more likely to be obtained using the harmonic method than with the amplitude and the phase shift methods due to a Fourier series. This result reflects the results of Otunla and Oladiran (2013). After a long period of drought, soil moisture content remained

close to the residual moisture (Fig. 2), with the movement of water in the sub-surface layer being slight. At this time, G_s from CCM had the largest *rRMSE*, value, though the influence of the soil moisture content is considered to simulate heat transport (Gao et al. 2003).

The results, however, are not always similar. During rainy conditions (Fig. 5c, d), the soil moisture content was high (Fig. 2), and the simulations using the four methods were worse than for clear-sky conditions. The main reason for this is believed to be because the soil temperature, in the absence of the daily steady wave, suddenly decreased due to the weather conditions, which is the first step to estimating k. Overestimation or underestimation in the simulation of the heat flux using the harmonic method resulted in *rRMSE* values being high, in contrast to Otunla and Oladiran (2013). Our results for the amplitude method, when compared to the results of the harmonic method, also indicated that this is not a suitable method to estimate k. CCM, being different from the other methods, because of the high soil moisture content (about 0.3 m^3 m^{-3}) may be the best method for estimating k and G_s on rainy days (Gao et al. 2003).

In overcast conditions, G_s closely reflects G_m despite inconsistencies between their phases, regardless of whether soil moisture content is high or low (Fig. 2). Although the harmonic method provides a good estimation of heat flux, the severe phase inconsistency results in poor *rRMSE* (Table 3). Therefore, the harmonic method is not recommended to estimate k in overcast conditions. Additionally, only one sine wave was used to fit the soil temperature, but CCM presented the best estimation under high soil moisture content. Gao et al. (2003) and Wang et al. (2010) emphasised that results from CCM are more accurate than those from the amplitude and the phase shift methods on the Tibet and the Loess Plateau experiments under clear-sky conditions. The CCM result from this study also concurs with that of Miao et al. (2012). When soil moisture content remains high (Fig. 5e, f), the phase shift method is an alternative to estimate k and G_s due to its small *rRMSE* and simple calculation. However, when the daily soil moisture content rapidly decreases (Fig. 5g, h), CCM is more accurate in estimating k.

Figure 6 shows the simulated heat flux G^* estimated by the gradient method with different k from the four methods (amplitude, phase shift, conduction–convection and harmonic) under different climatic conditions. The *rRMSE* between the heat fluxes G^* and G_m are shown in Table 4.

Generally, the heat flux G^* calculated by the gradient method with k from four methods (amplitude, phase shift, conduction–convection and harmonic) has a greater deviation from the measurements than does G_s. On rainy (Fig. 6c, d) or overcast days (Fig. 6e–h), the phase of G^* advanced that of G_m, which increases the estimation error. Conversely, the fluctuation of G^* is included while that of G_s is ignored. In addition, G^* is closer to the measured G_m than is G_s during the night.

The results, however, are sufficient to evaluate the accuracy of k from the four methods. It can be seen that the harmonic method is the best method to estimate k and G^* in clear-sky conditions, which is supported by Dai et al. (2009) and Miao et al. (2012) for arid soils. However, under rainy or overcast conditions, the harmonic method produces major errors. This is inconsistent with Otunla and Oladiran (2013). In addition, the *rRMSE* of the CCM is smaller than the other three methods under overcast conditions with high soil moisture content or with low soil moisture content but high water movement in the soil profile, a finding supported by Wang et al. (2010). The results have shown that the amplitude method should not be used to estimate k during or after rainy conditions as the heat flux is overestimated by 50 % when the soil is almost saturated; the higher soil moisture content restricts the application of the amplitude method to estimate k (Sellers 1965). Finally, because of small *rRMSE* values

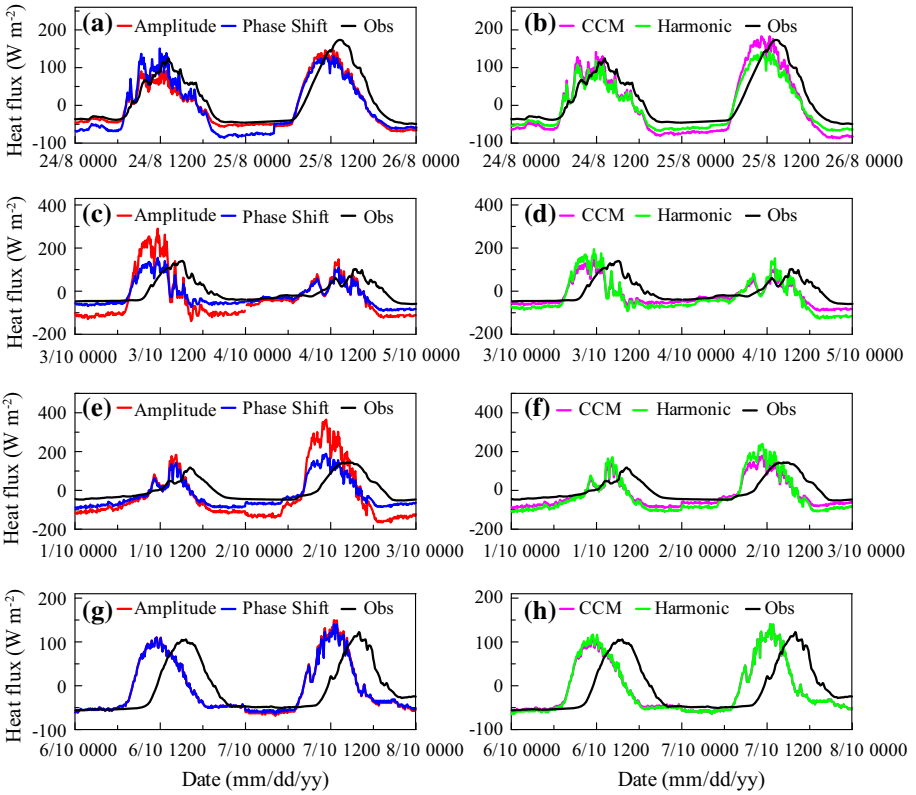

Fig. 6 Soil heat flux observed by heat-flux plates and estimated by the gradient method with different k from four methods at 0.03 m: **a**, **b** under clear conditions; **c**, **d** on rainy days; **e**, **f** under overcast conditions with high soil moisture content; and **g**, **h** under overcast conditions with low soil moisture content

Table 4 *rRMSE* of G^* estimated by the gradient method with four kinds of k against observations at 30 mm depth

Weather/method	Amplitude	Phase shift	CCM	Harmonic
Clear sky	2.47	2.34	3.17	2.43
Rainy	5.08	3.20	3.10	4.79
Overcast 1	4.48	2.58	2.49	3.30
Overcast 2	2.16	2.05	2.05	2.77

in overcast conditions, the phase shift is a reliable method to estimate k, instead of CCM, which avoids complex calculation.

Although G^* from the gradient method under different weather conditions is consistent with G_s from the amplitude, phase shift, conduction–convection and harmonic methods, the major discrepancy between G_m and G^* during daytime conditions generates a poor estimation of heat flux across the whole day. The gradient method, therefore, is not suitable to estimate heat flux based on the comparison between the experiment data and theoretical analysis.

Notably, the phase of G_s and G^* more or less advanced that of G_m under overcast and rainy conditions. This advance and discrepancy of G^* estimated by the gradient method is extremely severe when the movement of soil moisture content is high. There are three possible reasons that can explain this discrepancy. Firstly, the difference of the thermal conductivity between the heat-flux sensor and the soil cannot be ignored as a possible cause of this advance (Mogensen 1970; Heusinkveld et al. 2004). Secondly, the hypothesis of the heat conduction equation is that k, at adjacent depths, is constant. In reality, however, k is variable at different depths due to differing soil moisture content, soil shape and packing in the soil profile (Evett et al. 2012). Lastly, the deficiency of the four methods might result in the advance of phase. The deficiency is that only one value of k is deduced in the period of one day, however, daily soil moisture content affecting thermal parameters fluctuates at a certain depth, especially in overcast conditions (Fig. 2) when soil moisture content has decreased dramatically through the day.

5 Conclusions

To accurately estimate k under different weather conditions for the silty sand in north-west China, four methods (amplitude, phase shift, conduction–convection and harmonic) have been used. Heat fluxes estimated by these four methods and by the gradient method were also compared with measurements to validate the application of these methods.

Results show that there is no single method to accurately estimate k under differing weather conditions. Under clear-sky conditions, the harmonic method has a greater accuracy in estimating k than the amplitude and the phase shift methods in dry soils while CCM generates a major error in estimating k and heat flux when the soil is too dry. When the soil is wet, CCM is more accurate in estimating k than the amplitude, the phase shift and the harmonic methods under rainy or overcast conditions, while the accuracy of the harmonic and the amplitude methods is poor in estimating k under rainy conditions. By using a simple calculation, the phase shift is most suited to estimate k as a substitute for CCM under high soil moisture content conditions with low liquid movement.

When quantifying the heat transfer when coupling water, vapour and heat transfer in the soil, or the surface energy balance, different methods should be chosen to estimate k under different weather conditions. As estimating k is complex, the reason for the differences among these models is still unclear. Further investigation is needed, especially with respect to the energy balance.

Acknowledgments This study was supported by the Key Program of National Natural Science Foundation of China (no. 41230314) and Specialized Research Fund for the Doctoral Program of Higher Education of China (no. 20100205110007). The analysis was also partially supported by the program for Changjiang Scholars and Innovative Research Team of the Chinese Ministry of Education (IRT0811).

References

Abu-Hamdeh NH, Reeder RC (2000) Soil thermal conductivity effects of density, moisture, salt concentration, and organic matter. Soil Sci Soc Am J 64(4):1285–1290

Alkhaier F, Flerchinger GN, Su Z (2012) Shallow groundwater effect on land surface temperature and surface energy balance under bare soil conditions: modeling and description. Hydrol Earth Syst Sci 16(7): 1817–1831

Andry H, Yamamoto T, Irie T, Moritani S, Inoue M, Fujiyama H (2009) Water retention, hydraulic conductivity of hydrophilic polymers in sandy soil as affected by temperature and water quality. J Hydrol 373(1–2):177–183
Barrios M, Francés F (2012) Spatial scale effect on the upper soil effective parameters of a distributed hydrological model. Hydrol Proc 26(7):1022–1033
Bittelli M, Ventura F, Campbell GS, Snyder RL, Gallegati F, Pisa PR (2008) Coupling of heat, water vapor, and liquid water fluxes to compute evaporation in bare soils. J Hydrol 362(3–4):191–205
Carslaw HS, Jaeger JC (1959) Conduction of heat in solids. Clarendon Press, Oxford, 510 pp
Campbell GS (1985) Soil physics with BASIC: transport models for soil-plant systems, vol 14. Elsevier, Amsterdam
Dai CY, Gao ZQ, Wang LL, Fan JH (2009) Intercomparison between two soil temperature algorithms. J Atmos Sci Chinese 33(1):135–144
de Silans AMBP, Monteny BA, Lhomme JP (1996) Apparent soil thermal diffusivity, a case study: HAPEX-Sahel experiment. Agric For Meteorol 81(3–4):201–216
De Vries DA (1956) Thermal conductivity of soil. Nature 178:1074. doi:10.1038/1781074a0
Evett SR, Agam N, Kustas WP, Colaizzi PD, Schwartz RC (2012) Soil profile method for soil thermal diffusivity, conductivity and heat flux: comparison to soil heat flux plates. Adv Water Resour 50:41–54
Gao Z, Fan X, Bian L (2003) An analytical solution to one-dimensional thermal conduction-convection in soil. Soil Sci 168(2):99–107
Gao Z (2005) Determination of soil heat flux in a tibetan short-grass prairie. Boundary-Layer Meteorol 114(1):165–178
Heusinkveld B, Jacobs A, Holtslag A, Berkowicz S (2004) Surface energy balance closure in an arid region: role of soil heat flux. Agric For Meteorol 122(1):21–37
Hopmans J, Dane J (1986) Temperature dependence of soil hydraulic properties. Soil Sci Soc Am J 50(1):4–9
Horton R, Wierenga PJ (1983) Evaluation of methods for determining the apparent thermal diffusivity of soil near the surface. Soil Sci Soc Am J 47(1):25–32
Kunii D, Smith JM (1960) Heat transfer characteristics of porous rocks. AIChE J 6(1):71–78
Lin GF, Chen LH (2004) A non-linear rainfall-runoff model using radial basis function network. J Hydrol 289(1):1–8
Liu H, Wang B, Fu C (2008) Relationships between surface albedo, soil thermal parameters and soil moisture in the semi-arid area of Tongyu, northeastern China. Adv Atmos Sci 25(5):757–764
Miao YC, Liu SH, Lv SH, Zhang Y (2012) Study of computing methods of soil thermal diffusivity, temperature and heat flux. J Geophys Chin 55(2):441–451
Mogensen VO (1970) The calibration factor of heat flux meters in relation to the thermal conductivity of the surrounding medium. Agric Meteorol 7:401–410
Nerpin SV, Chudnovskii A, Powers WL (1972) Physics of the Soil. Am J Phys 40(6):926–926
Noborio K, McInnes K (1993) Thermal conductivity of salt-affected soils. Soil Sci Soc Am J 57(2):329–334
Otunla TA, Oladiran EO (2013) Evaluation of soil thermal diffusivity algorithms at two equatorial sites in West Africa. Ann Geophys 56(1):R0101
Riha SJ, McInnes K, Childs S, Campbell G (1980) A finite element calculation for determining thermal conductivity. Soil Sci Soc Am J 44(6):1323–1325
Saito H, Šimůnek J, Mohanty BP (2006) Numerical analysis of coupled water, vapor, and heat transport in the vadose zone. Vadose Zone J 5(2):784–800
Sellers WD (1965) Physical climatology. University of Chicago Press, Chicago, 272 pp
VAN Wijk WR (1963) Physics of plant environment. North Holland Publishing Company, Amsterdam, 382 pp
Verhoef A, van den Hurk BJ, Jacobs AF, Heusinkveld BG (1996) Thermal soil properties for vineyard (EFEDA-I) and savanna (HAPEX-Sahel) sites. Agric For Meteorol 78(1):1–18
Wang K, Wang P, Liu J, Sparrow M, Haginoya S, Zhou X (2005) Variation of surface albedo and soil thermal parameters with soil moisture content at a semi-desert site on the western Tibetan Plateau. Boundary-Layer Meteorol 116(1):117–129
Wang L, Gao Z, Horton R (2010) Comparison of six algorithms to determine the soil apparent thermal diffusivity at a site in the Loess Plateau of China. Soil Sci 175(2):51–60
Wang WK, Li JT, Feng XZ, Chen XH, Yao KJ (2011a) Evolution of stream-aquifer hydrologic connectedness during pumping-Experiment. J Hydrol 402(3):401–414
Wang WK, Zhao GZ, Li JT, Hou LL, Li YL, Yang F (2011b) Experimental and numerical study of coupled flow and heat transport. Water Manag 164:533–547
Wang L, Gao Z, Horton R, Lenschow DH, Meng K, Jaynes DB (2012a) An analytical solution to the one-dimensional heat conduction-convection equation in soil. Soil Sci Soc Am J 76(6):1978–1986

Wang WK, Dai ZX, Li JT, Zhou LL (2012b) A hybrid Laplace transform finite analytic method for solving transport problems with large Peclet and Courant numbers. Comput Geosci 49:182–189

Zhang Z, Wang W, Chen L, Zhao Y, An K, Zhang L (2015) Finite analytic method for solving the unsaturated flow equation. Vadose Zone J. doi:10.2136/vzj2014.06.0073

Zhao GZ, Wang WK, Hou LL, Li YL (2009) Determination of thermal parameter of aerated zone in the arid and semi-arid region. Hydrogeol Eng Chin 36(5):107–110